

Non-Line-Impedance-Synthesized Power Sharing Control in Microgrid Using On-Demand Power Feeding

Suchart Janjormanit ^{1*} Suttichai Premrudeepreechacharn ¹ Kohji Higuchi ²

¹ Chiang Mai University, 239, Huay Kaew Road, Mueang District, Chiang Mai 50300, Thailand

² The University of Electro-Communication, 1-5-1 Chofugaoka, Chofu, Tokyo 182-8585, Japan

*Corresponding author: Email: suchart@rmutl.ac.th

ABSTRACT

A method of power sharing control in the islanding operation of microgrid is proposed in this paper. The proposed approach formulates the power generation of each DG by the relationship of power-angle control, in which the magnitude and angle of the generating voltage are adjusted to follow the change of demanding power. By comparison to the previous work, the new method does not need the value of line impedance, connecting between DG and the common bus, to incorporate the control function. The method, limiting the output power and preventing power consumed by the DG, is also improved. The new method of power-angle control demonstrated that without using the knowledge of line impedance, the suitable power sharing point in the microgrid could also be tracked within each DG's capacity autonomously. Simulation and experimental results demonstrate the validity of the proposed control.

Keyword: Automatic generation control, distributed power generation, microgrids, power control, power sharing.

1. Introduction

Nowadays, microgrid is becoming a viable option for power generation since it distributes the autonomous energy supply. It provides a solution to the system where the energy demand is in the remote area and sometimes the power is disconnected from the public electricity. The Distributed Generation (DG) operated by power electronic converter, such as the Voltage Source Converter (VSC) , plays an important role in microgrid. In addition, the droop control technique is widely used for power sharing control in the islanding microgrid. In general, this technique

emulates the power generated by the synchronous generator where the output voltage magnitude and frequency are adjusted linearly to the power. There are studies on droop control with minimum communication between DGs [1]-[4]. The works on droop control without using additional communication [5]-[7] are also published. There are studies of the droop [8]-[9] published recently, but the works need the knowledge of line impedance to incorporate into the formulation of the control. Although the power sharing by the droop gains intensive implementation, it is proven to have limitations [10]-[11]. The control of power output

by varying voltage magnitude and frequency itself creates the residual deviation in the interconnected system. Angle droop [12]-[14] is proposed to eliminate the residual frequency deviation; however, in this method the power is still varied linearly with the voltage magnitude and angle by the droop equation. In addition, the operation relies on the Global Positioning System (GPS). There is also a study of GPS synchronized droop control [15] published recently, but the formulation of the control based on the assumption that the line impedance is known. The power sharing by droop is problematic to the system with resistive line impedance [6], [10]-[11], [16]-[19]. The concept of virtual impedance [20]-[22] has been proposed and successfully implemented to overcome this problem. The concept is actually the reference voltage modification that introduces the line impedance into the control loop. However, choosing of virtual impedance is complicated, it requires a trade-off between power sharing and voltage regulation [11]. The power sharing control by the droop has been used for a long time. Although this technique achieves high reliability and flexibility, it has several drawbacks that limit its application [11].

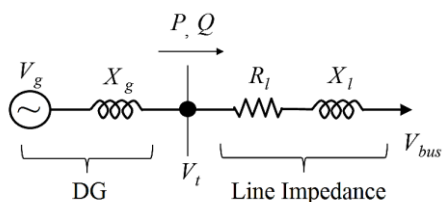


Fig. 1 Power delivery from DG to the bus.

In this research, the usage of droop control is eliminated. The idea of the power-angle control without incorporating the droop [23] is proposed firstly, but the method requires the value of line

impedance to formulate the control function. The limitation is further improved by this work.

2. Power Sharing Analysis

Fig. 1 shows the power delivery from DG via a line to its connected bus.

The active power generation [24], P , of the DG can be calculated by:

$$P = \frac{|V_g| |V_t|}{X_g} \sin(\delta_g) \quad (1)$$

where V_g is the generating voltage, V_t is the voltage at DG's terminal, δ_g is the angle between V_g and V_t , and X_g is output inductance of the DG. In addition, the reactive power generation [24], Q , can be calculated by:

$$Q = \frac{|V_t|}{X_g} (|V_g| \cos(\delta_g) - |V_t|) \quad (2)$$

The assumption is that the angle δ_g is small and it can be inferred from the above equations that increasing δ_g causes a greater change in active power than reactive power. In addition, the reactive power is changed depending on the difference in voltage magnitude between V_g and V_t , called ΔV .

3. The Proposed Power-Angle Control using On-demand Power Feeding

By using (1), the relationship between active power generation and the angle difference, δ_g , can be rewritten as:

$$\delta_g \approx \sin^{-1} \left(\frac{P X_g}{(|V_{bus}|^*)^2} \right) \quad (3)$$

To simplify the operation, the magnitude of voltage at bus $|V_{bus}|^*$ is used instead of V_g and V_t in (1), and it is treated as a constant value, as the rated voltage on the bus, to determine the required constraint operation of the DGs. In addition, by using (2) the relationship between

reactive power generation and the voltage difference, ΔV , can be rewritten as:

$$\Delta V \approx \frac{QX_g}{|V_{bus}|^*} \quad (4)$$

To simplify further, $\cos(\delta_g)$ is omitted due to the fact that the angle is small.

The power in (3) and (4) can be calculated in every voltage cycle or updating round by:

$$P^i = \frac{V_{max}I_{max} \cos(\theta)}{2} \quad (5)$$

$$Q^i = \frac{V_{max}I_{max} \sin(\theta)}{2} \quad (6)$$

where the superscript i indicates the number of consecutive cycle or round of update. θ is the angle of power factor. V_{max} and I_{max} are voltage and current magnitude detected at DG's terminal.

In order to control the power generation to follow the change of demanding power, the change of power from previous updating round, ΔP and ΔQ , needs to be detected, which can be calculated by:

$$\Delta P = P^i - P^{i-1} \quad (7)$$

$$\Delta Q = Q^i - Q^{i-1} \quad (8)$$

As it can be seen from (3) that the active power generation has a direct relationship to δ_g ; therefore, the control of active power generation by adjusting the angle difference δ_g can be calculated with:

$$\delta_g^i = \delta_g^{i-1} + \sin^{-1} \left(\frac{\Delta P X_g}{(|V_{bus}|^*)^2} \right) \quad (9)$$

The adjusting of the angle difference δ_g in this way is the determination to adjust the power sharing of each DG to the microgrid with the DG's constraint. The suitable power sharing point may not reach immediately, but rather for a number of updating rounds.

In addition, as it can be seen from (4) that the reactive power generation has a direct

relationship to ΔV ; therefore, the control of reactive power generation by adjusting the voltage difference P_m can be calculated by:

$$\Delta V^i = \Delta V^{i-1} + \frac{\Delta Q X_g}{|V_{bus}|^*} \quad (10)$$

The determination of the adjusting of ΔV in this way is also the same as the adjusting of δ_g in which it adjusts the power sharing of each DG to the microgrid with the DG's constraint.

Thus, in each round of updating cycle the reference voltage is generated by:

$$V_g(t) = (V_g^i + \Delta V^i) \sin(\omega t + \delta_g^i) \quad (11)$$

In order to avoid the exchanging power between DGs, or the power is consumed by the DG, the output power of each DG should be limited to its capacity. From Eq. (3), the maximum active power P_m can be translated into a maximum angle δ_{gm} , which can be expressed by:

$$\delta_{gm} \approx \sin^{-1} \left(\frac{P_m X_g}{(|V_{bus}|^*)^2} \right) \quad (12)$$

In each round of updating cycle, after the active power is detected, if the value of P is negative, δ_g is forced to increase a small degree (use +5% of δ_{gm} in this work), and if P is greater than its capacity, δ_g is forced to decrease a small degree as well (use -5% of δ_{gm} in this work). This creates a constraint of the power sharing to the microgrid so that the other DGs is perceived the limitation from the DG and the power generation is then adjusted in accordingly.

In the case of reactive power, the maximum reactive power Q_m is a maximum of voltage magnitude difference ΔV_m . From Eq. (4), it can be expressed by:

$$\Delta V_m \approx \frac{Q_m X_g}{|V_{bus}|^*} \quad (13)$$

In each round of updating cycle, after the reactive power is detected, if the value of Q is negative, V_g is forced to increase a small magnitude (use +5% of ΔV_m in this work), and if Q is greater than its capacity, V_g is forced to decrease a small magnitude as well (use -5% of

ΔV_m in this work). This also creates a constraint of the power sharing so that the other DGs is perceived and the power generation is then adjusted in accordingly too.

A flowchart of reference voltage generation is showed in Fig. 2 and Fig. 3 shows VSC using the

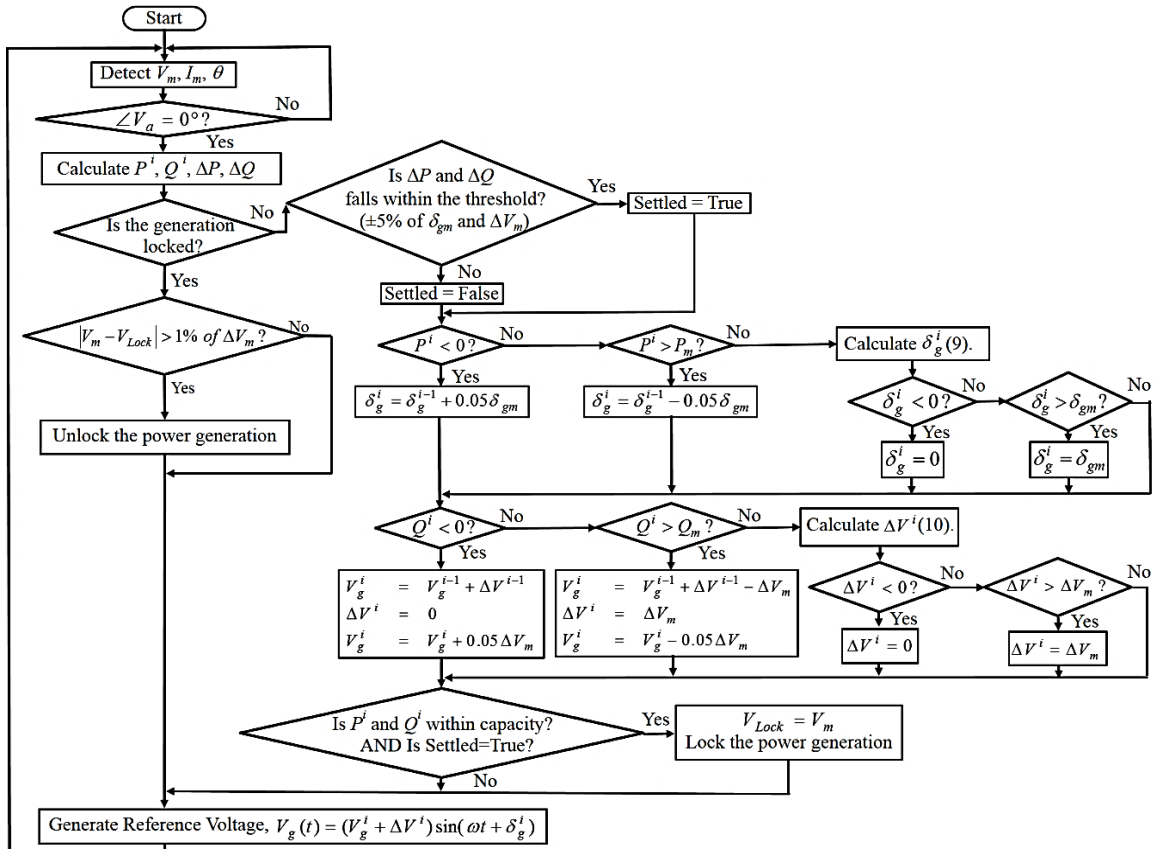


Fig. 2 Flowchart of the reference voltage generation.

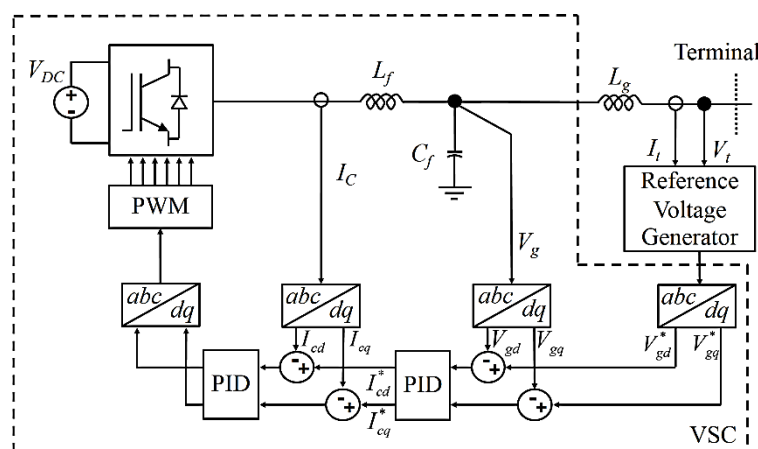


Fig. 3 A VSC with reference voltage generator.

reference voltage generator. The proposed analysis is based on the assumption that the load is balance. If the system is unbalanced, then all three lines need to be sensed and the proposed reference voltage generation may be formulated in the rotating d-q-0 coordinates, or at least the system should be separated to be three single- phase systems.

4. Simulation Studies

The simulation are performed using MATLAB /SIMULINK. The operation of the network is regarded as the islanding microgrid. The system is a 3-phase 380V/50Hz. The results are the locked values when the system is in the stable and steady-state power sharing point. All values are per unit with base MVA(1MVA) and the base kVLL(0.380). In order to compensate for voltage drop on the line, V_g at the beginning of the reference voltage generation should be higher than V_{bus} . In the simulations, V_g begins with 390V. In the simulation studies, the DG is simulated by ‘Controlled Voltage Source’ which means that there would not be voltage tracking error in the studies. The effect of voltage tracking error can be neglected when the error is minimal [23].

4.1. The Step Change of Load

Fig. 4 shows configuration of microgrid for this study. Table I gives parameters for systems under consideration.

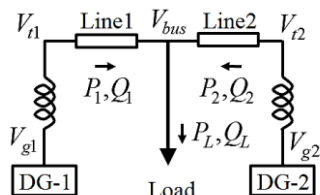


Fig. 4 Microgrid system under consideration.

TABLE I System parameters (step load change)

| Quantities | Values(pu) |
|---------------------|---|
| Line1 impedance | 0.125+j0.166 |
| Line2 impedance | 0.166+j0.208 |
| Load rating(before) | P=0.75, Q=0.05 |
| Load rating(after) | P=1.25, Q=0.1 |
| DG-1 rating | P _{m1} =0.75, Q _{m1} =0.1 |
| DG-2 rating | P _{m2} =0.75, Q _{m2} =0.1 |
| Output inductance 1 | j0.125 |
| Output inductance 2 | j0.125 |

The load begins by $P_L=0.75$ pu and $Q_L=0.05$ pu. The locked values before the load change are shown in Table II At 0.5 second, the load is step changed to $P_L=1.25$ pu. and $Q_L=0.1$ pu., and the simulation results during load changing are in Fig. 5(a) and 5(b). The simulation results of locked values after the load change are in Table III. The

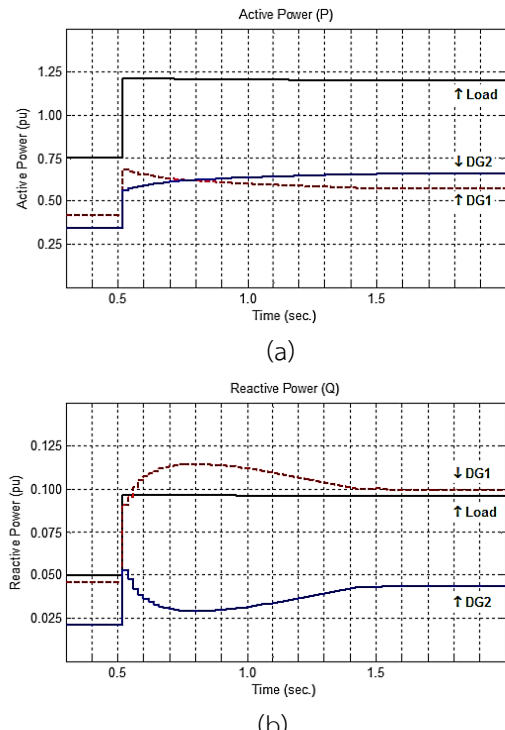


Fig. 5 Results of the step load change, (a) result of active power, and (b) result of reactive

results indicate that the approach is able to control the power generation even when the load is suddenly changed. In addition, it has to be noted in Fig. 5(b) that after the load change the reactive power of DG-1 are greater than its maximum capacity of 0.1, but the control is able to force the power down under its capacity.

TABLE II Results of step load change (before)

| Quantities | Values(pu) |
|------------------------|-----------------------------------|
| Result of DG-1 output | $P_1=0.421, Q_1=0.0458$ |
| Result of DG-2 output | $P_2=0.343, Q_2=0.0216$ |
| Result of load | $P_L=0.751, Q_L=0.0501$ |
| Volt. at bus | $V_{bus}=1.0039 \angle 0^\circ$ |
| Volt. at DG-1 output | $V_{g1}=1.0281 \angle 2.15^\circ$ |
| Volt. at DG-2 output | $V_{g2}=1.0271 \angle 2.05^\circ$ |
| Volt. at DG-1 terminal | $V_{t1}=1.0234 \angle 1.16^\circ$ |
| Volt. at DG-2 terminal | $V_{t2}=1.0237 \angle 1.22^\circ$ |

TABLE III Results of step load change (after)

| Quantities | Values(pu) |
|------------------------|-----------------------------------|
| Result of DG-1 output | $P_1=0.576, Q_1=0.1000$ |
| Result of DG-2 output | $P_2=0.659, Q_2=0.0431$ |
| Result of load | $P_L=1.198, Q_L=0.0994$ |
| Volt. at bus | $V_{bus}=0.9824 \angle 0^\circ$ |
| Volt. at DG-1 output | $V_{g1}=1.0195 \angle 2.71^\circ$ |
| Volt. at DG-2 output | $V_{g2}=1.0268 \angle 3.78^\circ$ |
| Volt. at DG-1 terminal | $V_{t1}=1.0113 \angle 1.93^\circ$ |
| Volt. at DG-2 terminal | $V_{t2}=1.0203 \angle 2.87^\circ$ |

4.2. Test of Meshed Network

Fig. 6 shows configuration of microgrid for consideration of meshed network. Table IV gives parameters for the system under consideration.

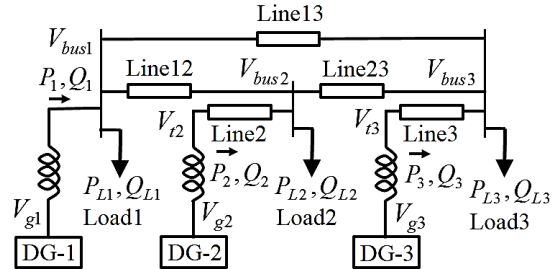


Fig. 6 Three-bus meshed network.

The simulation result of the three-bus meshed network are in Table V.

TABLE IV System parameters (meshed network)

| Quantities | Values(pu) |
|---------------------|-----------------------------------|
| Line1 impedance | - (Connected directly to the bus) |
| Line2 impedance | $0.166+j0.021$ |
| Line3 impedance | $0.332+j0.041$ |
| Line12 impedance | $0.166+j0.208$ |
| Line13 impedance | $0.021+j0.083$ |
| Line23 impedance | $0.125+j0.166$ |
| Load1 rating | $P=0.25, Q=0.05$ |
| Load2 rating | $P=0.5, Q=0.1$ |
| Load3 rating | $P=0.5, Q=0.05$ |
| DG-1 rating | $P_{m1}=0.5, Q_{m1}=0.1$ |
| DG-2 rating | $P_{m2}=1, Q_{m2}=0.2$ |
| DG-3 rating | $P_{m3}=0.75, Q_{m3}=0.1$ |
| Output inductance 1 | $j0.125$ |
| Output inductance 2 | $j0.125$ |
| Output inductance 3 | $j0.125$ |

It has been reported [11] that by far, the largest body of research work done in the decentralized microgrid control has been for radial network. The simulation results demonstrate that proposed method has a capability to control the power

sharing not only in the radial network, but also in the meshed network.

TABLE V Results of three-bus meshed network

| Quantities | Values(pu) |
|--------------------|-------------------------------------|
| DG-1 output | $P_1=0.455, Q_1=0.0978$ |
| DG-2 output | $P_2=0.511, Q_2=0.0633$ |
| DG-3 output | $P_3=0.285, Q_3=0.0394$ |
| Bus1 to bus2 | $P_{L12}=0.029, Q_{L12}=0.0096$ |
| Bus1 to bus3 | $P_{L13}=0.175, Q_{L13}=0.0389$ |
| Bus2 to bus3 | $P_{L23}=0.036, Q_{L23}=-0.0271$ |
| Result of load1 | $P_{L1}=0.246, Q_{L1}=0.0493$ |
| Result of load2 | $P_{L2}=0.491, Q_{L2}=0.0982$ |
| Result of load3 | $P_{L3}=0.491, Q_{L3}=0.0491$ |
| V at bus1 | $V_{bus1}=0.9961 \angle 0.26^\circ$ |
| V at bus2 | $V_{bus2}=0.9939 \angle 0.17^\circ$ |
| V at bus3 | $V_{bus3}=0.9939 \angle 0^\circ$ |
| V at DG-1 output | $V_{g1}=1.003 \angle 71.35^\circ$ |
| V at DG-2 output | $V_{g2}=1.0282 \angle 1.34^\circ$ |
| V at DG-3 output | $V_{g3}=1.0287 \angle 0.63^\circ$ |
| V at DG-1 terminal | $V_{t1}=0.9961 \angle 0.26^\circ$ |
| V at DG-2 terminal | $V_{t2}=1.0218 \angle 0.18^\circ$ |
| V at DG-3 terminal | $V_{t3}=1.0250 \angle -0.03^\circ$ |

5. Experimental Results

In order to prove that the concept has a feasibility to be implemented in real microgrid,

the proposed approach is tested in a down-scale single phase 220V/50Hz system.

Fig. 7 shows the configuration of the system of two DGs; all parameters are included in the figure. The system can be regarded as the system in Fig. 4. The parameters for the system in per unit with base kVA(0.3) and base kV(0.22), are in Table VI. To simplify the operation of the V_g tracking control, the V_g is controlled by a direct voltage-PWM control loop. The control functions of both DGs are operated by a single dSPACE system, but modules of the proposed power sharing control for each DG are separated.

There are problems related to the implementation of the VSC-type DG. The recommendation is given as follows for implementation of the proposed approach. If there are noisy environment, voltage fluctuation by controlling of VSC, and inaccuracy of the phase angle and peak detection, then the adjustment of power sharing by (9) and (10) may not be smooth and desirable. In order to mitigate those effects on power sharing, equation (9) and (10) need to be modified by adding a damping coefficient (C_d). Therefore, equation (9) is modified to be:

$$\delta_g^i = \delta_g^{i-1} + C_d \sin^{-1} \left(\frac{\Delta P X_g}{(|V_{bus}|^*)^2} \right) \quad (14)$$

, where equation (10) is modified as:

$$\Delta V^i = \Delta V^{i-1} + C_d \frac{\Delta Q X_g}{|V_{bus}|^*} \quad (15)$$

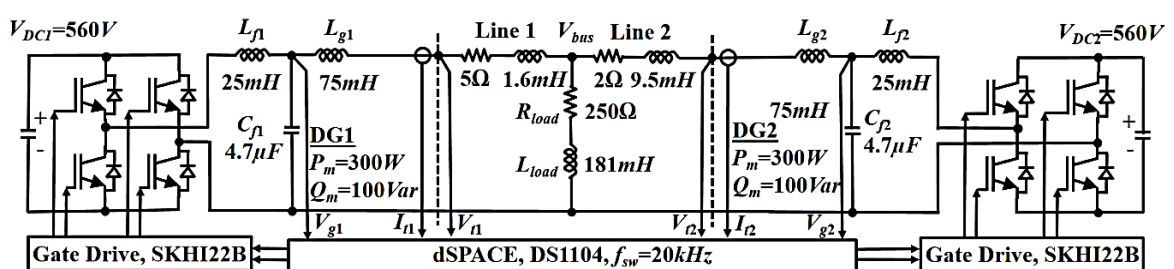


Fig. 7 Configuration of the experimental system.

The value of damping coefficient is between 0-1. For the system without any concerns about those effects, such as in the simulation study, C_d can be 1. The lower value of C_d is more mitigation of the effects on power sharing, but its response would be slower. In the experiment, it found that $C_d = 0.2$ is the optimal value in the test condition.

TABLE VI
System parameters (experimental system)

| Quantities | Values(pu) |
|---------------------|--------------------------|
| Line1 impedance | $0.0310+j0.0031$ |
| Line2 impedance | $0.0124+j0.0185$ |
| Load rating | $P=0.613, Q=0.138$ |
| DG-1 rating | $P_{m1}=1, Q_{m1}=0.333$ |
| DG-2 rating | $P_{m2}=1, Q_{m2}=0.333$ |
| Output inductance 1 | $j0.146$ |
| Output inductance 2 | $j0.146$ |

Table VII shows the results of the experiment in per unit and the parameters in the Table VI are the same values as in Fig. 7. Table VIII shows the results of the experiment of the previous work [23], in the same system. It can be noted that the results of power sharing are different between the two methods. This is due to the fact that the adjusting of V_g , ΔV and δ_g are different; whereas the previous work [23] need the value of line impedance to calculate the adjustment, this work does not need the value. The adjustment of each method leads to its own suitable power sharing point, which is different from each other.

6. Conclusions

This article proposes a method to control active and reactive power sharing in Microgrid. The proposed control is based on the power-angle control with on-demand power feeding. The presented technique is able to operate autonomously in islanding mode and in DG with either inductive or resistive line. The design of the control function is simple and it guarantees that there would not be the power consumed by the DGs. The experimental results show the validity that the proposed approach can be implemented in practices.

TABLE VII
Experimental results of the proposed method

| Quantities | Values(pu) |
|--------------------|----------------------------------|
| DG-1 output | $P_1=0.459, Q_1=0.016$ |
| DG-2 output | $P_2=0.161, Q_2=0.128$ |
| Result of load | $P_L=0.615, Q_L=0.140$ |
| Voltage at bus | $V_{bus}=1.0002\angle 0^\circ$ |
| V at DG-1 output | $V_{g1}=1.0173\angle 4.10^\circ$ |
| V at DG-2 output | $V_{g2}=1.0182\angle 1.73^\circ$ |
| V at DG-1 terminal | $V_{t1}=1.0141\angle 0.05^\circ$ |
| V at DG-2 terminal | $V_{t2}=1.0041\angle 0.08^\circ$ |

TABLE VIII
Experimental results of the previous work [23]

| Quantities | Values(pu) |
|--------------------|-----------------------------------|
| DG-1 output | $P_1=0.276, Q_1=0.003$ |
| DG-2 output | $P_2=0.343, Q_2=0.149$ |
| Result of load | $P_L=0.6166, Q_L=0.141$ |
| Voltage at bus | $V_{bus}=1.0032\angle 0^\circ$ |
| V at DG-1 output | $V_{g1}=1.0110\angle 1.96^\circ$ |
| V at DG-2 output | $V_{g2}=1.0296\angle 2.59^\circ$ |
| V at DG-1 terminal | $V_{t1}=1.0109\angle -0.35^\circ$ |
| V at DG-2 terminal | $V_{t2}=1.0100\angle -0.15^\circ$ |

7. Acknowledgements

This research was performed partly under the National Research University Project, Office of the Higher Education Commission, Thailand and Chiang Mai University. The authors would like to thank National Science and Technology Development Agency and Rajamangala University of Technology Lanna for scholarship and support for studying.

8. References

- [1] M. Prodanovic and T. C. Green, "High-quality power generation through distributed control of a power park microgrid," *IEEE Trans. Ind. Electron.*, vol. 53, no. 5, pp. 1471–1482, 2006.
- [2] M. N. Marwali, J. W. Jung, and A. Keyhani, "Control of distributed generation systems—Part II: Load sharing control," *IEEE Trans. Power Electron.*, vol. 19, no. 6, pp. 1551–1561, 2004.
- [3] A. Mehrizi-Sani and R. Iravani, "Potential function based control of a microgrid in islanded and grid-connected modes," *IEEE Trans. Power Syst.*, vol. 25, no. 4, pp. 1883–1891, 2010.
- [4] J. M. Guerrero, L. Hang, and J. Uceda, "Control of distributed uninterruptible power supply systems," *IEEE Trans. Ind. Electron.*, vol. 55, no. 8, pp. 2845–2859, 2008.
- [5] F. Katiraei and M. R. Iravani, "Power Management Strategies for a Microgrid with Multiple Distributed Generation Units," *IEEE Trans. Power Syst.*, vol. 21, no. 4, pp. 1821–1831, 2006.
- [6] J. M. Guerrero, J. Matas, L. G. de Vicuña, M. Castilla, and J. Miret, "Wireless-control strategy for parallel operation of distributed generation inverters," *IEEE Trans. Ind. Electron.*, vol. 53, no. 5, pp. 1461–1470, 2006.
- [7] K. D. Brabandere, B. Bolsens, J. V. D. Keybus, A. Woyte, J. Driesen, and R. Belmans, "A voltage and frequency droop control method for parallel inverters," *IEEE Trans. Power Electron.*, vol. 22, no. 4, pp. 1107–1115, 2007.
- [8] M. Ashabani, Y.A.-R.I. Mohamed, M. Mirsalim, and M. Aghashabani, "Multivariable droop control of synchronous current converters in weak grids/microgrids with decoupled dq-axes currents," *IEEE Trans. Smart Grid*, vol. 6, no. 4, pp. 1610-1620, 2015.
- [9] W. Ferreira de Souza, M.A. Severo-Mendes, and L.A.C. Lopes, "Power sharing control strategies for a three-phase microgrid in different operating condition with droop control and damping factor investigation," *IET Renewable Power Gener.*, vol. 9, no. 7, pp. 831-839, 2015.
- [10] J. Rocabert, A. Luna, F. Blaabjerg, and P. Rodríguez, "Control of power converters in AC microgrids," *IEEE Trans. Power Electron.*, vol. 27, no. 11, pp. 4734-4749, 2012.
- [11] J. M. Guerrero, M. Chandorkar, T. Lee, and P. C. Loh, "Advanced control architectures for intelligent microgrids—Part I: decentralized and hierarchical control," *IEEE Trans. Ind. Electron.*, vol. 60, no. 4, pp. 1254-1262, 2013.
- [12] R. Majumder, A. Ghosh, G. Ledwich and F. Zare, "Angle droop versus frequency droop in a voltage source converter based

autonomous microgrid," in IEEE Power & Energy Society General Meeting, Calgary, AB, 2009, pp. 1-8.

[13] R. Majumder, B. Chaudhuri, A. Ghosh, R. Majumder, G. Ledwich, and F. Zare, "Improvement of stability and load sharing in an autonomous microgrid using supplementary droop control loop," IEEE Trans. Power Syst., vol. 25, no. 2, pp. 796–808, 2010.

[14] R. Majumder, A. Ghosh, G. Ledwich, and F. Zare, "Load sharing and power quality enhanced operation of a distributed microgrid," IET Renewable Power Gener., vol. 3, no. 2, pp. 109–119, 2009.

[15] M. S. Golsorkhi and D. D. C. Lu, "A control method for inverter- Based islanded microgrids based on V- I droop characteristics," IEEE Trans. Power Delivery, vol. 30, no. 3, pp. 1196-1204, 2015.

[16] S. Tabatabaei, H. R. Karshenas, A. Bakhshai and P. Jain, "Investigation of droop characteristics and X/R ratio on small-signal stability of autonomous Microgrid," in The 2nd Power Electronics, Drive Systems and Technologies Conference, Tehran, 2011, pp. 223-228.

[17] J. M. Guerrero, L. GariadeVicuna, J. Matas, M. Castilla, and J. Miret, "Output impedance design of parallel- connected UPS inverters with wireless load-sharing control," IEEE Trans. Ind. Electron, vol. 52, no. 4, pp. 1126–1135, 2005.

[18] W. Yao, M. Chen, J. Matas, M. Guerrero, and Z. Qian, "Design and analysis of the droop control method for parallel inverters considering the impact of the complex impedance on the power sharing," IEEE Trans. Ind. Electron, vol. 58, no. 2, pp. 576–588, 2011.

[19] F. Z. Peng, Y. W. Li and L. M. Tolbert, "Control and protection of power electronics interfaced distributed generation systems in a customer-driven microgrid," in IEEE Power & Energy Society General Meeting, Calgary, AB, 2009, pp. 1-8.

[20] S. J. Chiang, C. Y. Yen, and K. T. Chang, "A multi module parallelable series-connected PWM voltage regulator," IEEE Trans. Ind. Electron, vol. 48, no. 3, pp. 506–516, 2001.

[21] Y. Xiaoxiao, A. M. Khambadkone, W. Huanhuan, and S. Terence, "Control of parallel- connected power converters for low- voltage microgrid— Part I: A hybrid control architecture," IEEE Trans. Power Electron, vol. 25, vo. 12, pp. 2962–2970, 2010.

[22] D. M. Vilathgamuwa, L. Poh Chiang, and Y. Li, "Protection of microgrids during utility voltage sags," IEEE Trans. Ind. Electron, vol. 53, no. 5, pp.1427–1436, 2006.

[23] S. Janjornmanit and S. Premrudeepreecharn, "A power sharing control for microgrid based on extrapolation of injecting power and power-angle control," Turk. J. Elec. Eng. & Comp. Sci., vol. 25, no. 2, pp. 689–704, 2017.

[24] W. D. Stevenson, *Elements of Power System Analysis*. Singapore, McGraw-Hill, 1982, pp. 206-208.